



Energy calibration of data recorded with the surface detectors of the Pierre Auger Observatory

CLAUDIO DI GIULIO¹ FOR THE PIERRE AUGER COLLABORATION²

¹ *Università and INFN di Roma II, "Tor Vergata", Via della Ricerca Scientifica 1,00133 Roma, Italy*

² *Observatorio Pierre Auger, Av. San Martín Norte 304, 5613 Malargüe, Argentina*

Claudio.DiGiulio@roma2.infn.it ICRC ID: 142 Date: April 1, 2009

Abstract: The energy of the primary particles of the air showers recorded using the water-Cherenkov detectors of the Pierre Auger Observatory is inferred from simultaneous measurement of the showers with the fluorescence telescopes. The signal on the ground at 1000 m from the shower axis obtained using the water-Cherenkov detectors is related directly to the calorimetric energy measured with the telescopes. The energy assignment is therefore independent of air-shower simulations except for the assumptions that must be made about the energy carried into the ground by neutrinos and muons. The correlation between the signal at ground and the calorimetric energy is used to derive a calibration curve. A detailed description of the method used to determine the energy scale is presented. The systematic uncertainties on the calibration procedure are discussed.

1 Introduction

2 The Pierre Auger Observatory [1] detect the
 3 air showers with the surface detector array
 4 composed by water-Cherenkov detectors with
 5 a 100% duty cycle [2]. The interpolated signal
 6 at a fixed optimal distance from the shower
 7 core, $S(1000)$ for the surface detector, is a good
 8 energy estimator in the sense that it is well
 9 correlated with the energy of the primary cosmic
 10 ray [3]. A subsample of the air showers is
 11 detected using simultaneously the fluorescence
 12 telescopes. They provides a nearly calorimetric
 13 energy measurement E_{FD} , because the fluorescence
 14 light is produced in proportion to energy
 15 dissipation by a shower in the atmosphere
 16 [4, 5]. This method can be used only
 17 when the sky is moonless and dark, and thus
 18 has about a 13% duty cycle [6]. For this
 19 subsample of air showers, called "hybrid events",
 20 it possible to relate the shower energy E_{FD}
 21 to the ground parameter $S(1000)$. The energy
 22 scale obtained studying this data sample is
 23 applied at the full sample of shower detected
 24 by the array of the water-Cherenkov detectors.

25 Data Analysis

In this analysis hybrid events collected by the
 Pierre Auger Observatory between the 1st of
 December 2004 and the 31st of May 2008 are
 used. To ensure that the shower is sampled to
 make an $S(1000)$ measurement with the surface
 array, the rejection of accidental triggers
 and the core of the shower contained inside the
 array are requested. The selection criteria used
 is that all six nearest neighbours of the station
 with the highest signal must be active.

A subset of high-quality hybrid events are
 selected requiring that, only events with the
 reconstructed zenith angle less than 60° are
 selected [7], the geometry of an event must be
 determined from the times recorded at a fluores-
 cence telescope, supplemented by the time at
 the water-Cherenkov detector with the highest
 signal and with the core of the shower within
 750 m from the shower axis [8]. It is also
 required that a reduced χ^2 is less than 2.5 for
 the fit of the longitudinal profile by Gaisser-
 Hillas function [9] and that the depth of shower

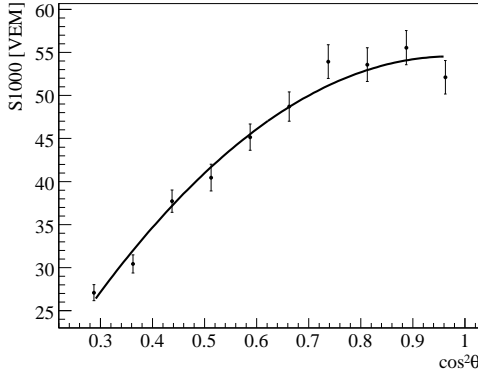


Figure 1: Derived attenuation curve, $CIC(\theta)$, fitted with a quadratic function.

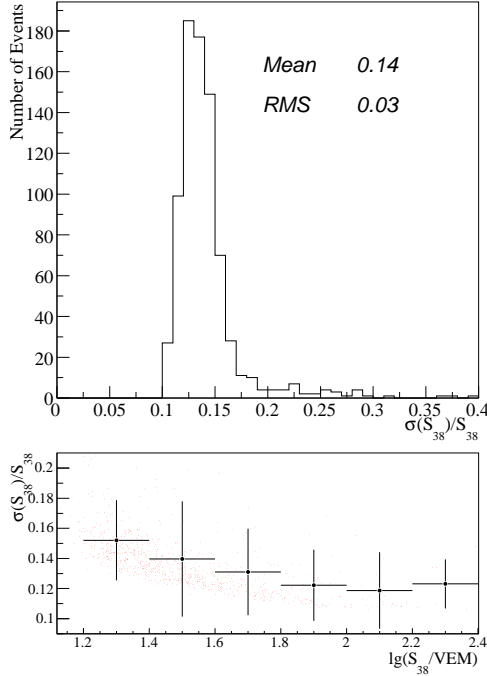


Figure 2: Upper panel: S_{38° resolution. Lower panel $\sigma_{S_{38^\circ}}/S_{38^\circ}$ on function of $\lg(S_{38^\circ}/VEM)$ scatter plot with mean profile.

48 maximum X_{\max} be within the field of view of
 49 the telescopes. The fraction of the signal attributed to Cherenkov light must be less than
 50 50%. The uncertainties on E_{FD} lower than
 51 20% and on X_{\max} lower than 40 g cm^{-2} are
 52 also requested. The selection criteria include
 53 a measurement of the vertical aerosol optical
 54 depth profile (VAOD(h)) [10] using laser
 55 shots generated by the central laser facility
 56 (CLF) [11] and observed by the fluorescence
 57 telescopes in the same hour of each selected
 58 hybrid event.

60 For a given energy the value of $S(1000)$ decreases with zenith angle, θ , due to attenuation
 61 of the shower particles and geometrical effects. Assuming an isotropic flux for the whole energy
 62 range considered, we extract the shape of the attenuation curve from the data [12]. The fitted
 63 attenuation curve, $CIC(\theta) = 1 + a x + b x^2$, is a quadratic function of $x = \cos^2 \theta - \cos^2 38^\circ$ as
 64 displayed in figure 1 for a particular constant intensity cut, that correspond to $S_{38^\circ} = 47 \text{ VEM}$,
 65 with $a = 0.91 \pm 0.05$ and $b = -1.28 \pm 0.23$. The average angle is $\langle \theta \rangle \simeq 38^\circ$ and we take this
 66 angle as reference and convert $S(1000)$ into S_{38° by $S_{38^\circ} \equiv S(1000)/CIC(\theta)$. It may be
 67 regarded as the signal $S(1000)$ the shower would have produced had it arrived at $\theta = 38^\circ$.

77 The reconstruction accuracy of the parameter $S(1000)$, $\sigma_{S(1000)}$ is composed by 3 contributions:
 78 a statistical uncertainty due to the finite
 79

80 size of the detector and the limited dynamic range of the signal detection, a systematic
 81 uncertainty due to the assumptions of the shape of the lateral distribution and finally due to
 82 the shower-to-shower fluctuations [13]. These are taken into account in inferring S_{38° and
 83 its uncertainty $\sigma_{S_{38^\circ}}$ and the relative uncertainty is about $\sigma_{S_{38^\circ}}/S_{38^\circ} = 14\%$ as shown in
 84 figure 2 and it is energy dependent.

85 Not all the energy of a primary cosmic ray particle ends up in the electromagnetic part of an
 86 air shower detected by fluorescence telescopes. Neutrinos escape undetected and muons need
 87 long path lengths to release their energy. This is usually accounted for by multiplying the
 88 electromagnetic energy by a correction factor f_{inv} determined from shower simulations to
 89 obtain the total primary energy. Due to the energy dependence of the meson decay probabilities
 90 in the atmosphere, and thus the neutrino and muon production probabilities, the

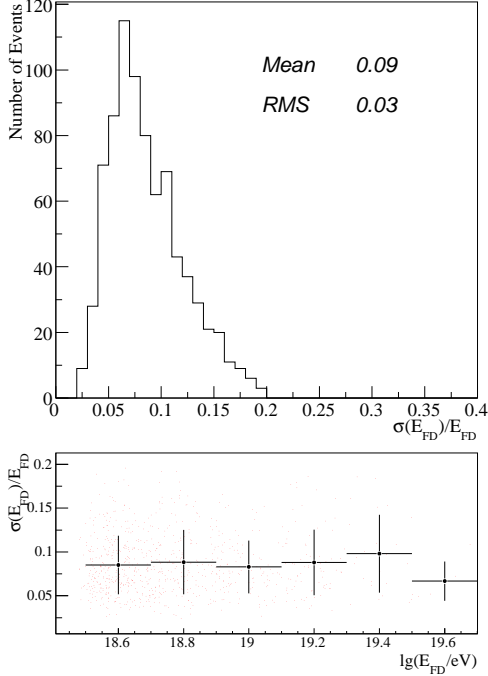


Figure 3: Upper panel: E_{FD} resolution. Lower panel $\sigma_{E_{FD}}/E_{FD}$ on function of $\lg(E_{FD}/\text{eV})$ scatter plot with mean profile.

101 correction depends on the energy for different
 102 hadronic interaction model, and is also subject
 103 to shower-to-shower fluctuations [14]. The so-
 104 called *invisible energy* correction is based on
 105 the average for proton and iron showers simu-
 106 lated with the QGSJet model and sums up to
 107 about 10%.

108 The statistical uncertainties of the total energy
 109 (E_{FD}) measured by the fluorescence tele-
 110 scopes ($\sigma_{E_{FD}}$) is composed by the statistical
 111 uncertainty of the light flux (σ_{flux}), the un-
 112 certainty due to the core location and shower
 113 direction (σ_{geo}), the uncertainty on the invis-
 114 ible energy correction (σ_{inv}) and the uncer-
 115 tainty related to the measured VAOD profile
 116 (σ_{atm}). The total relative uncertainty is about
 117 $\sigma_{E_{FD}}/E_{FD} = 9\%$ as shown in figure 3 and do
 118 not depend strongly on the energy measured in
 119 this energy range.

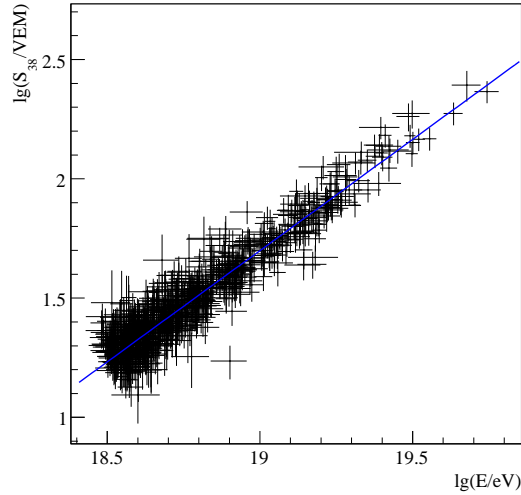


Figure 4: Correlation between $\lg(S_{38})$ and $\lg(E_{FD})$ for the 797 hybrid events used in the fit. The line is the best fit

120 Calibration Curve

121 The 797 hybrid selected events in the energy
 122 region where the surface detectors array is full
 123 efficiency ($E \geq 3 \text{ EeV}$), appear to be well de-
 124 scribed by a power-law: $E = a S_{38}^b$ as shown
 125 in figure 4. The results of the fit are:

$$126 a = (1.51 \pm 0.06(\text{stat}) \pm 0.12(\text{syst})) \times 10^{17} \text{ eV},$$

$$127 b = 1.07 \pm 0.01(\text{stat}) \pm 0.04(\text{syst}),$$

128 with a reduced χ^2 of 1.01. S_{38} grows approx-
 129 imately linearly with energy. The root-mean-
 130 square deviation of the distribution is about
 131 17% as shown in figure 5, in good agreement
 132 with the quadratic sum of the S_{38}° and E_{FD}
 133 statistical uncertainties. The calibration accu-
 134 racy at the highest energies is limited by the
 135 number of events: the most energetic is about
 136 $6 \times 10^{19} \text{ eV}$. The calibration at low energies
 137 extends below the range of interest.

138 Systematic Uncertainties

139 The systematics uncertainty due to the cali-
 140 bration procedure are 7% at 10^{19} eV and 15%
 141 at 10^{20} eV . At this uncertainty the systematic
 142 uncertainty due to the fluorescence telescope
 143 energy measurements must be considered.

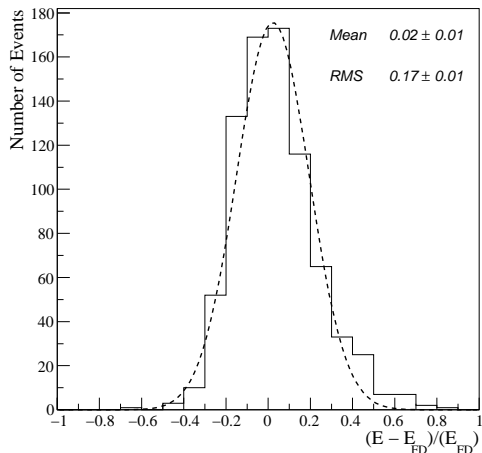


Figure 5: Fractional difference between the calorimetric energy (E_{FD}) and surface detector energy (E) obtained by the calibration curve, for the 797 selected events.

The individual systematic uncertainties in determining E coming from the FD sum up to 22%. The largest uncertainties are given by the absolute fluorescence yield (14%) [15], the absolute calibration of the fluorescence telescopes (9%) and the uncertainty due to the reconstruction method of the longitudinal shower profile (10%).

The uncertainty due to the dependence of the fluorescence spectrum on pressure (1%), humidity (5%) and temperature (5%) are taken into account as well as the wavelength dependent response of the fluorescence telescopes, the aerosol phase function and others, which are well below 4%. The *invisible energy* correction introduces a systematic uncertainty contributing 4% at the total systematic of 22% [16].

Outlook

The energy calibration of the surface detectors array obtained with the fluorescence telescopes with a detailed study of the uncertainties is given. The systematic uncertainties dominate, and several activities are on-going to reduce the systematic uncertainties of the

energy estimate, e.g. the longitudinal profile reconstruction method and the uncertainty of the fluorescence yield. The spectrum obtained by the surface detectors data calibrated with the method presented is compared with a spectrum derived on basis of hybrid data only in F. Schuessler et al. [17].

References

- [1] J. Abraham [Pierre Auger Collaboration], NIM 523 (2004) 50.
- [2] T. Suomijarvi [Pierre Auger Collaboration] Proc. 30th ICRC, Merida, (2007), #0299.
- [3] A. M. Hillas, Acta Physica Academiae Scientiarum Hungaricae Suppl. 3 **29** (1970), 355.
- [4] M. Risse and D. Heck, Astropart. Phys. 20 (2004) 661.
- [5] H. Barbosa et al., Astropart. Phys. 22 (2004) 159.
- [6] F. Salamida [Pierre Auger Collaboration] these proceedings, (2009) #0XXX.
- [7] D. Allard [Pierre Auger Collaboration], Proc. 29th ICRC, Pune (2005), **7**, 71.
- [8] L. Perrone [Pierre Auger Collaboration] Proc. 30th ICRC, Merida, (2007), #0316.
- [9] M. Unger *et al.*, Nucl. Instr. and Meth. **A 588**, 433 (2008).
- [10] S. Ben-Zvi [Pierre Auger Collaboration] Proc. 30th ICRC, Merida, (2007) #0399.
- [11] B. Fick et al., JINST, 1 (2006) 11003.
- [12] J. Hersil et al. Phys. Rev. Lett. **6**, 22 (1961).
- [13] M. Ave [Pierre Auger Collaboration] Proc. 30th ICRC, Merida, (2007), #0297.
- [14] T. Pierog et al., Proc. 29th ICRC, Pune (2005).
- [15] M. Nagano, K. Kobayakawa, N. Sakaki, K. Ando, Astropart. Phys. 22 (2004) 235.
- [16] B. Dawson [Pierre Auger Collaboration] Proc. 30th ICRC, Merida, (2007), #0976.
- [17] F. Schuessler [Pierre Auger Collaboration] these proceedings, (2009) #0XXX.